Decoupling the Image Perception and Multimodal Reasoning for Reasoning Segmentation with Digital Twin Representations

Yizhen Li
liyizhen@mail.sdu.edu.cn
ShanDong University
China

Dell Zhang
dell.z@ieee.org
TeleAI, China Telecom
China

Xuelong Li
xuelongli@ieee.org
TeleAI, China Telecom
China

Yiqing Shen*
yshen92@jhu.edu
Johns Hopkins University
America

ABSTRACT

Reasoning Segmentation (RS) is a multimodal vision-text task that requires segmenting objects based on implicit text queries, demanding both precise visual perception and vision-text reasoning capabilities. Current RS approaches rely on fine-tuning vision-language models (VLMs) for both perception and reasoning, but their tokenization of images fundamentally disrupts continuous spatial relationships between objects. We introduce DTwinSeger, a novel RS approach that leverages Digital Twin (DT) representation as an intermediate layer to decouple perception from reasoning. Innovatively, DTwinSeger reformulates RS as a two-stage process, where the first transforms the image into a structured DT representation that preserves spatial relationships and semantic properties and then employs a Large Language Model (LLM) to perform explicit reasoning over this representation to identify target objects. We propose a supervised fine-tuning method specifically for LLM with DT representation, together with a corresponding fine-tuning dataset Seg-DT, to enhance the LLM's reasoning capabilities with DT representations. Experiments show that our method can achieve state-of-the-art performance on two image RS benchmarks and three image referring segmentation benchmarks. It yields that DT representation functions as an effective bridge between vision and text, enabling complex multimodal reasoning tasks to be accomplished solely with an LLM.

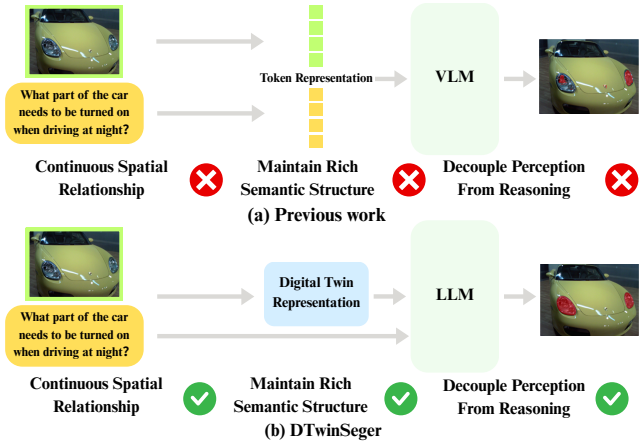

Figure 1: Comparison of image reasoning segmentation approaches. (a) Previous VLM-based methods fail to maintain continuous spatial relationships between objects during tokenization, compromise rich semantic structures, and inadequately separate perception from reasoning processes. (b) Our proposed DTwinSeger approach introduces DT representation as an intermediate layer that preserves spatial relationships and semantic structure while effectively decoupling perception (handled by DT representation) from reasoning (performed by LLM).

CCS CONCEPTS

• **Computing methodologies** → **Image representations**.

KEYWORDS

Reasoning Segmentation, Vision-Language Reasoning, Digital Twin Representation

1 INTRODUCTION

Reasoning Segmentation (RS) [19, 40] is a challenging vision-text multimodal task that requires models to segment objects based on implicit text queries through complex reasoning processes.

Unlike referring segmentation tasks [17, 21, 23, 43], that rely on direct references, RS demands more complicated cross-modal understanding to interpret semantic relationships, spatial contexts,

, ,

ACM ISBN XXX-X-XXXX-XXXX-X/25/10…$15.00
https://doi.org/XXXXXXX.XXXXXXX

and implicit attributes that are suggested in natural language instructions. Current RS approaches [4, 8, 19, 34–36, 38, 40, 41] are based on fine-tuned vision language models (VLMs), which attempt to handle both perception and reasoning. For instance, LISA [19] connects a VLM [2, 3, 20, 21, 26–28] (*e.g.*, LLaVA [21]) with a segmentation model (*e.g.*, SAM [18]) by utilizing special token embeddings to generate masks based on user instructions. However, the tokenization of images in VLMs for perception inevitably disrupts the continuous spatial relationships between objects, compromising the rich semantic structure necessary for complex cross-modal reasoning and resulting in suboptimal performance.

To address these limitations, we introduce the Digital Twin (DT) representation [7, 13, 22] to serve as an intermediate layer. Our major innovation lies in extending this concept, which is traditionally used in industrial and engineering contexts, to the multimodal reasoning domain. Compared to token-based RS counterparts, such as LISA [19], our DT representation can maintain a continuous semantic space that preserves spatial relationships between objects, enabling perception to be decoupled from reasoning. Based on the DT representation, we propose a novel image RS method, named DTwinSeger, by reformulating RS as a two-stage process. DTwinSeger first transforms the image into a structured DT representation that preserves all spatial and semantic information for perception, then employs a Large Language Model (LLM) [1, 10, 16, 32] to perform explicit reasoning over it. As shown in Fig. 1, DTwinSeger innovatively transforms RS from a VLM-dependent fine-tuning task to an LLM-agnostic framework, where the perception component is handled by the DT representation, and reasoning occurs through transparent LLM operations. To further improve the reasoning stage, we propose a supervised fine-tuning on digital twin representation (SFTDT) method with a corresponding Seg-DT dataset, demonstrating the generalization capability across multiple RS benchmarks.

The major contributions are three-fold. First, we introduce a method for constructing DT representations from images by combining mask proposal generation with semantic tagging. Our approach uses a hierarchical segmentation strategy that categorizes the output into object group, object, and object part levels, with specialized processing for each level. This construction process preserves both spatial relationships and semantic properties while providing a structured representation suitable for explicit reasoning. Second, we propose DTwinSeger, an RS approach that decouples perception from reasoning using our DT representation as an intermediate layer between vision and text for multimodal reasoning segmentation. Third, we propose SFTDT, a supervised fine-tuning method that enhances LLMs' reasoning capabilities on DT representations. Finally, we introduce Seg-DT, a fine-tuning DT representation dataset for LLM.

2 RELATED WORKS

2.1 Reasoning Segmentation

Reasoning Segmentation (RS) [19, 40] is a multimodal vision-text task that predicts the masks of target objects inferred from implicit text queries. Unlike traditional segmentation tasks, RS demands cross-modal understanding and reasoning to interpret semantic relationships, spatial contexts, and implicit attributes suggested in natural language instructions. Current RS methods are primarily based on token representation and typically require fine-tuning VLMs [4, 8, 19, 34–36, 38, 40, 41]. LISA [19] links VLMs with segmentation models by prompting the decoder with special token embeddings to generate masks corresponding to objects referenced in user instructions. However, this tokenization of images may disrupt the continuous spatial relationships between objects, which can undermine the model's ability to maintain the rich semantic structure. CoReS [4] implements a dual-chain architecture that connects VLMs with segmentation models using separate reasoning and segmentation chains, progressively interpreting and localizing visual elements in complex user queries. However, it still operates within the token representation for the image and can exhibit reduced accuracy when processing intricate queries that require complex spatial reasoning. GSVA [38] attempts to address multi-object scenes by generating multiple [SEG] tokens and introduces a [REJ] token to handle empty target situations. Similarly to other token-based approaches, GSVA suffers from the limitation of image tokenization, which disrupts the spatial continuity between objects. A common limitation across these token-based representations for image preception is their inability to maintain continuous spatial relationships during the tokenization process. This compromises the preservation of rich semantic structures that are important for complex cross-modal reasoning in RS. Furthermore, these methods do not adequately separate perception from reasoning processes, potentially leading to suboptimal performance in scenarios requiring sophisticated visual understanding. To overcome these limitations, we introduce the DT representation [7, 13, 22] as an intermediate layer. Unlike the aforementioned token-based RS approaches, such as LISA [19], CoReS [4], and GSVA [38], our DT representation preserves a continuous semantic space that maintains spatial relationships between objects, allowing perception to be decoupled from reasoning.

2.2 Digital Twins

Digital Twin (DT) [7, 13, 22] enables automatic cyclic data flows between physical objects and their digital counterparts. NASA defined it as "an integrated simulation that uses physical models, sensor updates, and history to mirror its corresponding twin" [14]. DT can also be conceptualized as "an outcome-driven paradigm creating a dynamic digital replica of a physical process". DT representations is the building block of DT, which is formally defined as the "outcome-driven digital representations extracted from raw data". Unlike token representations, DT representations can preserve semantic and physical relationships while maintaining domain-specific constraints [39]. DT has been adopted across various domains. For example, in manufacturing, previous work [5] demonstrated how DTs enable collaborative assembly of humans and robots. In smart cities, previous work [25] showed that DTs can model urban infrastructure for efficient resource management. Healthcare applications include Twin-S for skull base surgery [31] and surgical data science frameworks [11]. Although DT has demonstrated benefits across domains, our work pioneers its application to the field of reasoning segmentation. By encoding images as DT representations that capture spatial relationships and semantic properties, these representations function as effective bridges between vision and text,

enabling complex multimodal reasoning tasks to be accomplished simply with an LLM.

3 METHODS

3.1 Construction of Digital Twin Representation

The DT representation serves as an intermediate layer in our DTwinSeger framework, bridging the gap between visual perception and textual reasoning in RS. The construction of DT representation involves two main stages, namely, generating mask proposals that preserve spatial information and assigning semantic attributes that enable explicit reasoning. It begins with a hierarchical mask generation that addresses the challenges of segmentation granularity. Formally, we identify three distinct segmentation granularities, namely (1) object group level (involving multiple related objects), (2) object level (corresponding to complete individual objects), and (3) object part level (representing specific components of objects). We employ a VLM [2, 3, 20, 21, 26–28] ($\mathcal{F}_{\text{VLM}}$) to determine the appropriate segmentation granularity L for a given task based on the input image x_{img} and text query x_{txt}, namely

$$L = \mathcal{F}_{\text{VLM}}(x_{\text{img}}, x_{\text{txt}}), \tag{1}$$

where $L \in \{0, 1, 2\}$, with $L = 0$ indicating object group level, $L = 1$ indicating object level and $L = 2$ for object part level. Since the object group level can be conceptualized as multiple object level results, we implement the same mask proposal generation approach for the object group level and object level, with additional processing for the object part level. Specifically, for mask proposal generation, we utilize the Segment Anything Model (SAM) with "everything" mode [18]. For the image x_{img} of dimensions $H \times W$, we uniformly sample $N = 32 \times 32 = 1024$ points, each point serving as an independent prompt to generate a single mask with SAM [18]. The mask generation process can be formalized as $\{m_1, m_2, ..., m_N\} = \text{SAM}_{\text{everything}}(x_{\text{img}})$, where $\{m_1, m_2, ..., m_N\}$ denotes the set of masks generated initially. To address redundancy and ensure mask quality, we design a filtering mechanism based on SAM's predicted IoU values. We filter out masks with low predicted IoU using a threshold θ, namely $M_{\text{filtered}} = \{m_i | \text{IoU}_{\text{pred}}(m_i) > \theta\}$. For the object part level, we further refine the masks by computing the IoU between each pair of masks m_i and m_j, that is, $\text{IoU}(m_i, m_j) = \frac{|m_i \cap m_j|}{|m_i \cup m_j|}$. When $\text{IoU}(m_i, m_j) > \tau$, where τ is a predetermined threshold, we remove one of the overlapping masks to reduce redundancy. For object level and object group level processing, we compute the centroid c_i of each mask m_i, *i.e.*

$$c_i = \left(\frac{1}{|m_i|} \sum_{(x,y) \in m_i} x, \frac{1}{|m_i|} \sum_{(x,y) \in m_i} y \right). \tag{2}$$

These centroids serve as prompts for the SAM decoder in "multi-mask" mode [18]. Then, we identify the largest mask m^* as $m^* = \arg\max_{m_i} A(m_i)$, where $A(m_i)$ represents the area of mask m_i. For each remaining mask m_j, we compute the intersection ratio:

$$R(m_j) = \frac{|m_j \cap m^*|}{|m_j|}. \tag{3}$$

If $R(m_j) > \tau'$, where τ' is another predetermined threshold, we discard mask m_j to obtain more coherent object-level segmentation results. A computational advantage of our DT representation construction method is that while there are 1024 point prompts for SAM, the computationally intensive image encoder operates only once, with the lightweight mask decoder processing these prompts in batches. To accommodate large images within GPU memory constraints, we adjust the batch size during inference. The entire mask proposal generation stage requires approximately 6.5 seconds per image on a single NVIDIA RTX 4090 GPU.

Afterward, the semantic assignment stage is important for enabling explicit reasoning in RS. We extend beyond merely labeling objects by integrating the semantics of the query with contextual information from surrounding objects in the image. For each mask m_i obtained from the mask proposal stage, we crop it from the original image x_{img} and, together with the text query x_{txt}, apply VLM [2, 3, 20, 21, 26–28] $\mathcal{F}_{\text{VLM}}$ to derive appropriate semantics, depicted as

$$S_i = \mathcal{F}_{\text{VLM}}(x_{\text{img}}, x_{\text{txt}}, m_i, \{m_j\}_{j \neq i}), \tag{4}$$

where S_i represents the semantic information assigned to mask m_i, and $\{m_j\}_{j \neq i}$ denotes the set of all other masks that provide contextual information. Consequently, the final DT representation D of x_{img} integrates spatial (masks) and semantic information as $D = \{(i, m_i, S_i) | i = 1, 2, \ldots, N'\}$, where $N' \leq N$ is the number of masks selected after filtering, i is the index of the object, m_i represents the spatial information (mask) of the object, and S_i denotes the corresponding semantic information.

3.2 Reasoning Segmentation on DT Representation

After constructing the DT representation, DTwinSeger transforms RS into a pure language-based reasoning task over structured DT representations, as shown in Fig. 2, which effectively decouples perception from reasoning. Formally, the input to the LLM consists of the DT representation $D = \{(i, m_i, S_i) | i = 1, 2, \ldots, N'\}$ and the text query x_{txt}. Since LLMs cannot directly process image data, we convert spatial information m_i into textual descriptions of object locations, sizes, and spatial relationships with other objects. For each object, we include its bounding box coordinates $b_i = (x_{\min}, y_{\min}, x_{\max}, y_{\max})$, where $x_{\min}, y_{\min}$ represents the top-left corner and $x_{\max}, y_{\max}$ represents the bottom-right corner of the bounding box. We also compute the area A_i of each mask m_i, expressed as a percentage of the total area of the mask. We then encode relative spatial relationships $R_{i,j}$ between objects using positional descriptors, namely $R_{i,j} = \mathcal{T}(m_i, m_j, x_{\text{img}})$ where $\mathcal{T}$ is a transformation function that converts the spatial relationship between masks m_i and m_j into natural language descriptors (*e.g.*, "to the left of", "above," "inside," "surrounding"). The complete textual representation of the spatial information for an object is $T_i == \mathcal{F}_{\text{spatial}}(b_i, A_i, \{Ri, j\}_{j \neq i})$, where $\mathcal{F}_{\text{spatial}}$ is a predefined text template that better wraps up this information. The complete DT representation is formatted as a structured JSON object with the following format:

$$\text{JSON}(D) = \{i : \{\text{"spatial"} : T_i, \text{"semantic"} : S_i\}\}. \tag{5}$$

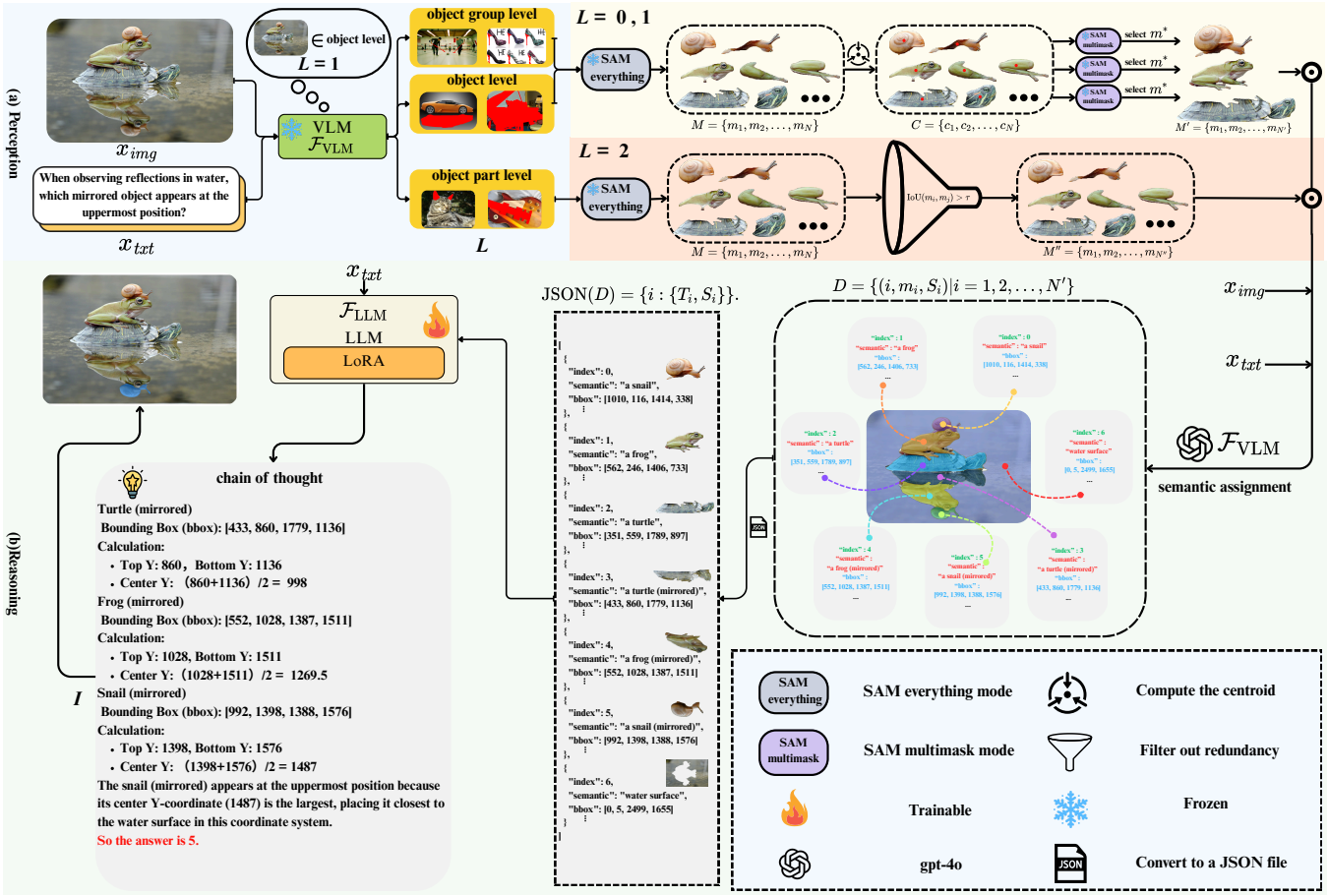

Figure 2: Illustration of our DTwinSeger. It consists of two main stages: (a) DT representation construction and (b) reasoning segmentation. In the DT construction stage, a VLM $\mathcal{F}_{\text{VLM}}$ first analyzes the image x_{img} and text query x_{txt} to determine the appropriate segmentation granularity L (object group, object, or object part level). For object group and object levels, SAM's "everything" mode generates initial masks followed by "multimask" mode using center points c_i for refinement. For object part level, SAM's "everything" mode is used with IoU-based filtering to remove overlapping masks. The semantic assignment process then integrates object properties with contextual information into semantic descriptions S_i, creating a structured JSON-format DT representation. In the reasoning stage, an LLM processes the DT representation to perform explicit reasoning over the structured data, either in zero-shot manner or through our SFTDT approach that employs chain-of-thought reasoning with progressive refinement. The final output is a set of object indices I corresponding to objects that satisfy the query, which are mapped back to segmentation masks for the final result.

The LLM [1, 10, 16, 32] processes this structured representation to determine which objects satisfy the text query x_{txt}. The output is a set of indices $I = i | i \in 1, 2, \ldots, N'$ and object i satisfies x_{txt} corresponding to objects that meet the text query. These indices can then be mapped back to their corresponding masks $\mathcal{M} = \{m_i | i \in I\}$ to generate the final segmentation result, that is, $m_{\text{out}} = \bigcup_{m \in \mathcal{M}} m$. Formally, RS with DT representation can be formulated as:

$$I = \mathcal{F}_{\text{LLM}}(\text{JSON}(D), x_{\text{txt}}) \tag{6}$$

where $\mathcal{F}_{\text{LLM}}$ represents the LLM that takes the JSON format of DT representation D and text query x_{txt} as input and outputs the set of object indices I. Note that the LLM in Eq. (6) supports both zero-shot and fine-tuned LLMs for reasoning over DT representations.

3.3 Supervised Fine-tuning on Digital Twin Representation

To better adapt LLM to Eq. (6), we propose supervised fine-tuning on DT representation, which can enhance LLMs' reasoning capabilities for processing DT representations through chain-of-thought reasoning [37, 42, 45]. The major innovation of SFTDT lies in that it progressively refines the DT representation according to the text query requirements. Rather than directly predicting the final object indices, the SFTDT trains the LLM to produce a reasoning path $\mathcal{P} = \{D^{(0)}, D^{(1)}, \ldots, D^{(K)}\}$ represented as a sequence of intermediate DT representations, where $D^{(0)} = D$ is the initial DT representation, and $D^{(K)}$ contains only objects that satisfy the text

query x_{txt}. Each transition from $D^{(j-1)}$ to $D^{(j)}$ involves filtering objects and refining their semantic descriptions based on the text query, namely

$$D^{(j)} = \mathcal{F}_{\text{refine}}(D^{(j-1)}, x_{\text{txt}}), \tag{7}$$

where $\mathcal{F}_{\text{refine}}$ refinement that evaluates objects against the text query and updates their semantic descriptions of the objects based on LLM. Specifically, $D^{(j)} = \{(i, m_i, S_i^{(j)}) | i \in \mathcal{I}^{(j)}\}$, where $\mathcal{I}^{(j)} \subseteq \mathcal{I}^{(j-1)}$ is the set of object indices retained after the j-th refinement step, and $S_i^{(j)}$ is the updated semantic information that explicitly relates the object to the query criteria. The refinement process for each intermediate step can be formally defined as:

$$\begin{aligned} \mathcal{I}^{(j)} &= \{i | i \in \mathcal{I}^{(j-1)} \text{ and } C(i, x_{\text{txt}}, D^{(j-1)}) = 1\} \\ S_i^{(j)} &= \mathcal{U}(S_i^{(j-1)}, x_{\text{txt}}, D^{(j-1)}) \end{aligned} \tag{8}$$

where C is a binary prediction based on LLM that determines whether the object i satisfies the criteria in step j based on the text query and the current representation of DT, and $\mathcal{U}$ is an update based on LLM that enriches the semantic description to include reasoning-specific information. The JSON format of each intermediate DT representation $D^{(j)}$ is structured to facilitate explicit reasoning $\text{JSON}(D^{(j)}) = \{i : \{\text{"spatial"} : T_i, \text{"semantic"} : S_i^{(j)}, \text{"reasoning"} : R_i^{(j)}\}\}$, where $R_i^{(j)}$ is a new field that explicitly captures the reasoning process for object i at step j, explaining why the object is retained or rejected based on the text query.

SFTDT fine-tunes the LLM to generate these intermediate reasoning steps and the final set of object indices:

$$(\mathcal{P}, I) = \mathcal{F}_{\text{LLM}}^{\text{SFTDT}}(\text{JSON}(D), x_{\text{txt}}), \tag{9}$$

where $\mathcal{F}_{\text{LLM}}^{\text{SFTDT}}$ represents the fine-tuned LLM that takes the JSON format of the DT representation D and the text query x_{txt} as input and outputs both the reasoning path $\mathcal{P}$ and the set of object indices I. The fine-tuning process employs a next-token prediction objective with a modified cross-entropy loss function that places higher weight on tokens associated with reasoning decisions and final indices:

$$\mathcal{L} = -\sum_t w_t \log P(y_t | \text{JSON}(D), x_{\text{txt}}, y_{<t}), \tag{10}$$

where y_t is the target token at position t, $y_{<t}$ represents all preceding tokens, and w_t is the weight assigned to token t based on its role in the reasoning process. We use LoRA [12, 15] when optimizing Eq. (10) to save the computation cost.

3.4 Fine-tuning Data Construction

To implement our SFTDT approach, we develop the Seg-DT dataset specifically designed to train LLMs for RS. The dataset construction process focuses on creating high-quality training examples that demonstrate the progressive reasoning path required for complex multimodal reasoning in vision-text tasks. The Seg-DT dataset consists of carefully curated input-output pairs structured to support chain-of-thought reasoning over DT representations. For each training example, the input comprises the JSON-formatted DT representation $\text{JSON}(D)$ paired with a text query x_{txt}. The output includes both the intermediate reasoning path $\mathcal{P} = \{D^{(0)}, D^{(1)}, \ldots, D^{(K)}\}$ and the final set of object indices I that satisfy the query requirements. We begin the data set construction process by selecting diverse images and generating challenging text queries that require various levels of complexity of reasoning. For each pair of image and query, we first construct the complete DT representation $D = \{(i, m_i, S_i) | i = 1, 2, \ldots, N'\}$ following the approach described previously. To ensure the quality of the DT representation, we apply a filtering mechanism based on predicted IoU values, creating $D_{\text{filtered}} = \{(i, m_i, S_i) | i \in \{1, 2, \ldots, N'\}$ and $\text{IoU}_{\text{pred}}(m_i) \geq \tau\}$ where τ is a predefined IoU threshold that ensures the spatial accuracy of the masks. For each filtered DT representation, domain experts manually annotate the reasoning path $\mathcal{P}$ and the final set of object indices I. The annotation of the reasoning path involves creating a sequence of intermediate DT representations $\{D^{(0)}, D^{(1)}, \ldots, D^{(K)}\}$ where $D^{(0)} = D_{\text{filtered}}$ is the initial filtered DT representation. Each successive $D^{(j)}$ reflects the progressive refinement of objects and their semantic descriptions, with $D^{(K)}$ containing only objects that satisfy the text query x_{txt}. For each intermediate step, the annotators provide $D^{(j)} = \{(i, m_i, S_i^{(j)}, R_i^{(j)}) | i \in \mathcal{I}^{(j)}\}$ where $\mathcal{I}^{(j)} \subseteq \mathcal{I}^{(j-1)}$ is the set of object indices retained after the j-th refinement step, $S_i^{(j)}$ is the updated semantic information, and $R_i^{(j)}$ explicitly documents the reasoning process for object i in step j. The final set of ground truth indices is determined as $I = \mathcal{I}^{(K)} = \{i | i \in \{1, 2, \ldots, N'\}$ and object i satisfies $x_{\text{txt}}\}$. To ensure dataset diversity and quality, we incorporate reasoning tasks across different segmentation granularities (object group level, object level, and object part level).

4 EXPERIMENTS

4.1 Experimental Setting

Implementation Details. The SFTDT was performed for 5 epochs using a learning rate of 2×10^{-5} with a cosine learning rate scheduler and gradient accumulation steps of 8. Training the entire framework took approximately 17 hours using 8 NVIDIA RTX 4090 GPUs. For inference, the DT representation construction takes approximately 6.5 seconds per image on a single RTX 4090 GPU. For VLMs used in a zero-shot manner, we utilize GPT-4o [27]; for the SFTDT, we employ Llama-3.3-70B [29] as the backbone. The mask proposal generation stage employs SAM [18] with a ViT-H backbone.

Datasets. Our Seg-DT data set for fine-tuning contains 239 samples in total. Evaluations are performed on both reference segmentation datasets (RefCOCO [43], RefCOCO+ [43] and RefCOCOg [23]) and image reasoning segmentation datasets (ReasonSeg [19] and LLM-Seg40K [33]). The ReasonSeg benchmark comprises 1,218 samples partitioned into train, validation, and test splits with 239, 200, and 779 samples, respectively [19]. The LLM-Seg40K dataset contains 14K images divided into training (11K), validation (1K), and test (2K) sets [33]. For all of these datasets, we only use their validation and test splits for evaluation. For reference segmentation datasets, we evaluate standard splits, including validation, TestA and TestB for RefCOCO/RefCOCO+, and validation (U) and test (U) for RefCOCOg [23, 43], following the setting of LISA [19].

Evaluation Metrics. We employ two metrics, namely the global Intersection over Union (gIoU) and composite Intersection over

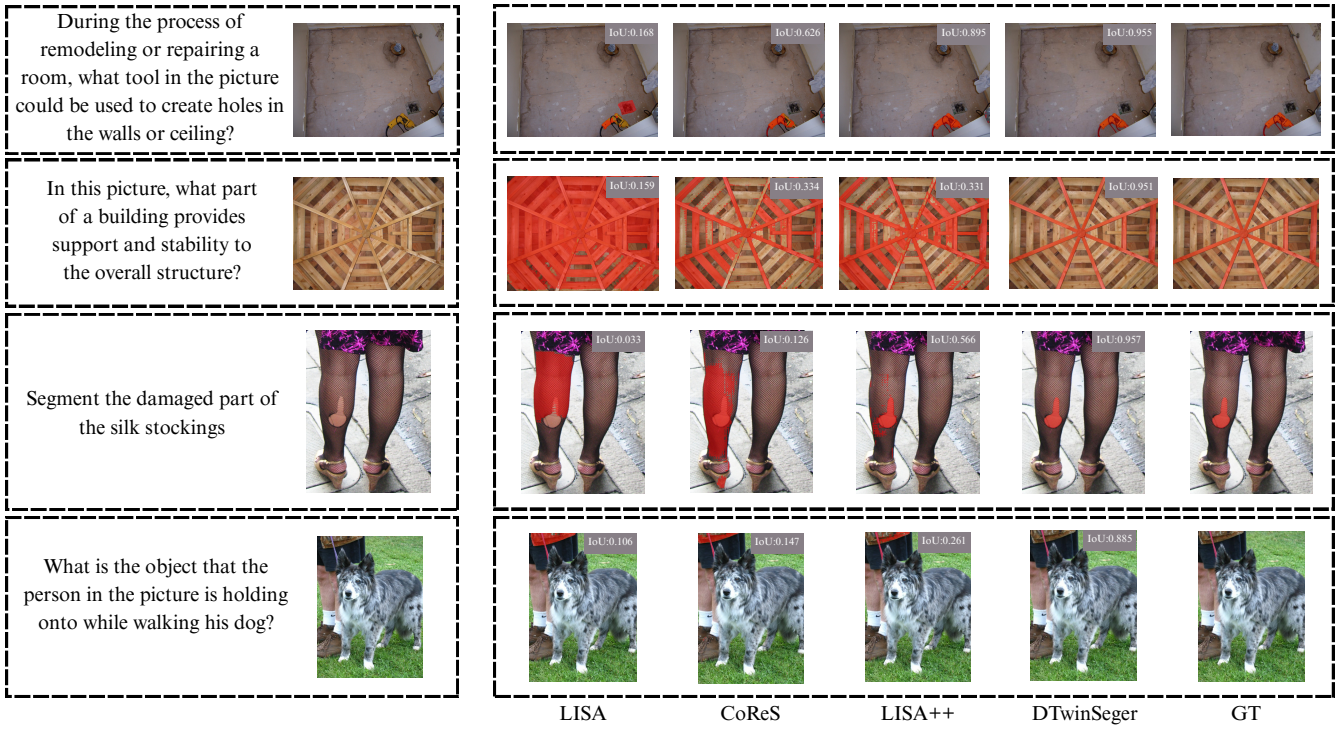

Figure 3: Illustrative examples of the reasoning segmentation performance with LISA, LISA++, CoReS, our proposed DTwinSeger, and ground truth (GT) across four reasoning queries from ReasonSeg test dataset. DTwinSeger consistently produces masks that more closely align with ground truth.

Table 1: Performance comparison of DTwinSeger against state-of-the-art methods on the ReasonSeg dataset. Results demonstrate that both zero-shot DTwinSeger and fine-tuned DTwinSeger (ft) with our SFTDT method outperform existing methods across all evaluation settings.

Method	Val		Test (short query)		Test (long query)		Test (overall)	
	gIoU	cIoU	gIoU	cIoU	gIoU	cIoU	gIoU	cIoU
CoReS [4]	61.8	62.4	49.7	50.2	58.3	59.1	55.9	56.4
LaSagnA [36]	45.1	47.2	40.2	41.1	42.2	42.4	42.5	43.6
LISA [19]	61.3	62.9	48.3	46.3	57.9	59.7	55.6	56.9
LISA++ [40]	64.2	68.1	49.6	51.1	59.3	61.7	57.0	59.5
LLM-Seg [33]	55.4	45.6	42.7	41.9	51.7	50.2	49.9	48.5
SAM4MLLM [8]	58.4	60.4	43.6	45.9	54.3	55.9	52.1	53.0
SegLLM [35]	57.2	54.3	43.8	42.5	51.9	51.8	50.9	49.5
DTwinSeger	**65.4**	**71.1**	**63.3**	**69.1**	**64.7**	**70.6**	**64.4**	**70.2**
DTwinSeger (ft)	**73.1**	**72.4**	**69.7**	**70.3**	**71.6**	**70.9**	**70.5**	**70.6**

Union (cIoU) [30, 44]. The gIoU metric represents the mean of individual image-level IoU scores, which capture performance uniformly across all samples regardless of object size [30]. In contrast, cIoU aggregates total intersection and union areas across the entire dataset, which inherently weights larger objects more heavily [44].

4.2 Comparison on ReasonSeg Dataset

Our proposed DTwinSeger approach demonstrates superior performance when compared to state-of-the-art methods on the ReasonSeg dataset. As shown in Table 1, both the zero shot DTwinSeger and the fine-tuned DTwinSeger with SFTDT consistently outperform existing approaches in all evaluation settings. In the validation set, our zero-shot DTwinSeger achieves 65.4% gIoU and 71.1% cIoU, surpassing the previous best performer, LISA++ (64.2% gIoU and 68.1%

cIoU). When fine-tuned with SFTDT, DTwinSeger further improves performance to 73.1% gIoU and 72.4% cIoU, representing gains of 8.9% and 4.3% in gIoU and cIoU, respectively, over LISA++ [40]. Performance improvement is also observable in the test set, where the zero-shot DTwinSeger achieves 63.3% gIoU and 69.1% cIoU on short queries, and 64.7% gIoU and 70.6% cIoU on long queries. These results significantly outperform the previous best method (LISA++ [40]) by 13.7% gIoU and 18.0% cIoU for short queries, and 5.4% gIoU and 8.9% cIoU for long queries. In general, on the test set, zero-shot DTwinSeger achieves 64.4% gIoU and 70.2% cIoU, representing absolute improvements of 7.4% gIoU and 10.7% cIoU over LISA++ [40]. With fine-tuning, DTwinSeger further widens this performance gap, achieving 69.7% gIoU and 70.3% cIoU on short queries, 71.6% gIoU and 70.9% cIoU on long queries, and 70.5% gIoU and 70.6% cIoU overall on the test set. These results represent substantial improvements of 13.5% gIoU and 11.1% cIoU in overall test performance compared to LISA++ [40]. Furthermore, Fig. 3 provides an illustrative comparison; and Fig. 4 provides a case study that demonstrates how our approach effectively decouples perception (handled by DT construction) from reasoning (performed by the LLM). Substantial performance gains can be attributed to our novel DT representation, which effectively bridges vision and text modalities by preserving spatial relationships and semantic structures. Our approach decouples perception from reasoning, allowing specialized components to handle each task optimally. Furthermore, the SFTDT method enhances the LLM's reasoning capabilities over DT representations, particularly evident in the consistent performance improvements across both short and long queries.

Table 2: Performance comparison of DTwinSeger against state-of-the-art methods on the LLM-Seg40K dataset.

Method	Val		Test	
	gIoU	cIoU	gIoU	cIoU
CoReS [4]	43.52	50.81	41.68	47.69
LISA [19]	43.16	50.79	41.23	47.33
LISA++ [40]	44.18	51.14	41.97	48.26
LLM-Seg [33]	45.47	54.18	43.25	51.60
SAM4MLLM [8]	43.29	49.65	42.35	48.97
DTwinSeger	**52.74**	**57.77**	**50.82**	**54.71**
DTwinSeger (ft)	**54.68**	**58.92**	**51.97**	**55.81**

4.3 Comparison on LLM-Seg40K Dataset

Table 2 presents the evaluation of DTwinSeger in the LLM-Seg40K dataset [33]. In the validation set, DTwinSeger achieves 52.74% gIoU and 57.77% cIoU, exceeding the next best competitor (LLM-Seg [33]) by 7.27% and 3.59%, respectively. This pattern extends to the test set, where DTwinSeger records 50.82% gIoU and 54.71% cIoU, surpassing LLM-Seg by 7.57% in gIoU and 3.11% in cIoU. Further enhancements emerge when our supervised fine-tuning method is applied, which pushes the performance boundaries to 54.68% gIoU and 58.92% cIoU on the validation set, while achieving 51.97% gIoU and 55.81% cIoU on the test set. The consistent superiority of DTwinSeger across different datasets highlights the robustness of our DT representation as an effective intermediary between visual perception and language-based reasoning. By preserving spatial relationships and semantic information in a structured format accessible to LLMs, our approach enables a more accurate interpretation of complex vision-text queries. Notably, while traditional VLM-based methods face limitations due to their tokenization processes that disrupt spatial continuity, our DT representation maintains these important relationships, facilitating more precise reasoning in segmentation.

4.4 Comparison on Referring Segmentation Datasets

Table 3: Performance comparison of DTwinSeger against state-of-the-art methods on referring segmentation benchmarks in terms of cIoU.

Method	**refCOCO** [43]			**refCOCO+** [43]			**refCOCOg** [23]	
	Val	TestA	TestB	Val	TestA	TestB	Val (U)	Test (U)
GSVA [38]	79.2	81.7	77.1	70.3	73.8	63.6	75.7	77.0
CoRes [4]	76.0	78.6	72.5	65.1	70.0	58.6	69.0	70.7
LaSagnA [36]	76.8	78.7	73.8	66.4	70.6	60.1	70.6	71.9
LISA [19]	74.9	79.1	72.3	65.1	70.8	58.1	67.9	70.6
LLaVaSeg [41]	76.2	79.1	72.9	65.7	71.4	57.7	69.8	70.1
SAM4MLLM [8]	79.8	82.7	74.7	74.6	78.8	67.2	75.5	76.4
DTwinSeger	**79.8**	**82.9**	**76.6**	**75.4**	**78.8**	**69.4**	**76.6**	**77.1**
DTwinSeger (ft)	**80.0**	**83.1**	**78.9**	**77.5**	**79.5**	**70.2**	**77.4**	**78.1**

Table 3 presents our evaluation of DTwinSeger on referring segmentation benchmarks (refCOCO, refCOCO+, and refCOCOg) [23, 43], which focus on direct referential expressions rather than complex reasoning requirements. Our DTwinSeger still demonstrates strong performance across all datasets, achieving competitive or superior results compared to specialized referring segmentation methods. Specifically, on refCOCO, DTwinSeger achieves 79.8%, 82.9%, and 76.6% cIoU on Val, TestA, and TestB splits, respectively, matching or exceeding all competing methods except where it outperforms most but falls slightly behind GSVA [38]. For refCOCO+, DTwinSeger records 75.4%, 78.8%, and 69.4% cIoU across the respective splits, surpassing most competitors except SAM4MLLM [8] on TestA. On refCOCOg, our approach achieves 76.6% and 77.1% cIoU on validation and test sets, outperforming all previous methods. When enhanced with our SFTDT method, DTwinSeger further enhances performance across all benchmark datasets, achieving state-of-the-art results on every data set split. These results validate that the benefits of our DTwinSeger framework extend beyond complex reasoning segmentation to more straightforward referring tasks, demonstrating its versatility as a general-purpose approach for vision-text multimodal segmentation.

4.5 Ablation Study

We conduct an ablation study to evaluate the contribution of each component in our DTwinSeger. Table 4 presents the quantitative results on the ReasonSeg validation set. For mask proposal generation in DT construction stage, we compare three strategies: (1) using the SAM's "everything" mode directly without adjustments, (2) fine-tuning SAM parameters for different granularity levels,

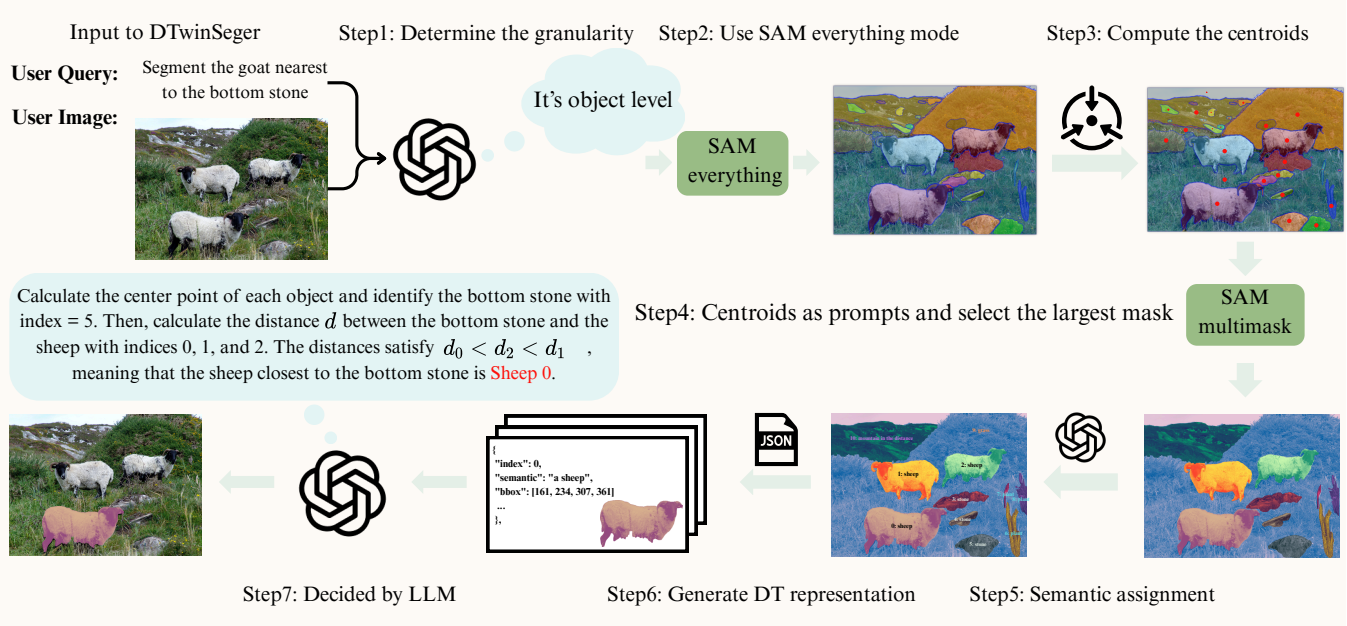

Figure 4: Step-by-step illustration of the DT representation construction process in DTwinSeger. First, a VLM determines the appropriate segmentation granularity, then SAM in "everything' mode generates initial mask proposals. Center points are calculated for each detected object, which serve as prompts for SAM in "multimask" mode to generate refined masks, with the largest mask selected. The semantic assignment is applied to each object. Finally, a structured DT representation is created that preserves both spatial relationships and semantic properties. The LLM performs reasoning over the DT representation.

Table 4: Ablation studies using ReasonSeg dataset on different components of DTwinSeger.

Component	Configuration	gIoU	cIoU
Mask Proposal	SAM only	37.6	34.5
	SAM with fine-tuning	40.4	41.1
	SAM + VLM refinement	**65.4**	**71.1**
Semantic Assignment	OWLv2 [24]	27.6	24.5
	VLM-based	**65.4**	**71.1**
VLM Prompting	Direct Query	50.6	50.2
	In-context Learning [6, 9]	59.4	60.0
	System-level Prompting	**65.4**	**71.1**
VLM	GPT-4o-mini [26]	60.1	59.0
	Qwen2.5-VL-72B [3]	63.7	65.5
	GPT-4o [27]	**65.4**	**71.1**

and (3) our hierarchical approach that uses both SAM and VLM refinement with specialized processing for different mask levels. The results show that our hierarchical approach with VLM refinement outperforms the other methods, improving gIoU by 27.8% and cIoU by 36.6%, compared to using SAM alone. This confirms the importance of our mask granularity differentiation strategy, which effectively handles different object levels (object group, object, and object part). We evaluate two semantic assignment approaches for the DT construction: (1) using open-vocabulary object detection (OWLv2 [24]) combined with SAM [18], where we first detect main objects with OWLv2 and then assign semantic labels to the corresponding masks, and (2) our VLM-based approach that directly assigns semantics to mask proposals. Our VLM-based semantic assignment demonstrates superior performance, achieving 65.4% gIoU and 71.1% cIoU, compared to 27.6% gIoU and 24.5% cIoU from the OWLv2. This improvement validates our design choice of using VLMs for semantic assignment, which provides more accurate semantic information in DT representation. The prompt engineering strategy for VLM interactions affects performance. We experiment with three prompting strategies: (1) direct query, where we directly ask the model to describe the semantics, (2) in-context learning, where we provide specific examples for the model to learn semantic assignment patterns, and (3) system-level prompting, which implements a brainstorming workflow where the VLM first summarizes its observations and then selects the optimal semantic assignment. The system-level prompting strategy achieves the best performance, outperforming the direct query by 14.8% in gIoU and 20.9% in cIoU, demonstrating its effectiveness. We also investigate the impact of different VLMs on the performance of DTwinSeger. We compare GPT-4o-mini [27], Qwen2.5-VL-72B, and GPT-4o [26]. Although GPT-4o-mini [26] offers computational efficiency, it achieves lower performance (60.1% gIoU and 59.0% cIoU). Qwen2.5-VL-72B delivers competitive results but still falls short of GPT-4o [27]. The complete GPT-4o [27] model demonstrates the best performance (65.4% gIoU and 71.1% cIoU), confirming our selection for the final framework.

5 CONCLUSION

We present DTwinSeger, a novel RS framework that introduces DT representation as an effective intermediate layer between visual perception and textual reasoning. Unlike existing RS approaches that rely on token-based VLMs for both perception and reasoning, our method decouples these processes, preserving continuous spatial relationships and rich semantic structures that are essential for complex cross-modal understanding. The major innovation of DTwinSeger lies in reformulating reasoning segmentation as a two-stage process. It transforms images into structured DT representations that maintain all spatial and semantic properties and then leverages LLMs to perform explicit reasoning over these representations. Our DT representation specific supervised fine-tuning method (SFTDT) with the corresponding Seg-DT dataset further enhances the reasoning capabilities of LLM on DT representation. Experimental results confirm that DTwinSeger outperforms current state-of-the-art methods on both reasoning segmentation datasets and referring segmentation benchmarks. As multimedia applications increasingly demand cross-modal understanding, DTwinSeger provides a promising direction for developing a more capable and transparent multimodal reasoning framework. One future direction can explore the extension of DT representations to video domains together with the improvement of real-time processing for practical multimedia applications. Another direction can be the integration of our approach into mixed reality environments where precise object segmentation and spatial reasoning are important for creating seamless interactions between virtual and physical elements.

REFERENCES

[1] Alibaba DAMO Academy. 2025. Qwen 2.5: The Next-Generation Open-Source Large Language Model. https://github.com/QwenLM/Qwen2.5

[2] Jean-Baptiste Alayrac, Jeff Donahue, et al. 2022. Flamingo: A Visual Language Model for Few-Shot Learning. *arXiv preprint arXiv:2204.14198* (2022). https://arxiv.org/abs/2204.14198

[3] Shuai Bai, Keqin Chen, Xuejing Liu, Jialin Wang, Wenbin Ge, Sibo Song, Kai Dang, Peng Wang, Shijie Wang, Jun Tang, Humen Zhong, Yuanzhi Zhu, Mingkun Yang, Zhaohai Li, Jianqiang Wan, Pengfei Wang, Wei Ding, Zheren Fu, Yiheng Xu, Jiabo Ye, Xi Zhang, Tianbao Xie, Zesen Cheng, Hang Zhang, Zhibo Yang, Haiyang Xu, and Junyang Lin. 2025. Qwen2.5-VL Technical Report. arXiv:2502.13923 [cs.CV] https://arxiv.org/abs/2502.13923

[4] Xiaoyi Bao, Siyang Sun, Shuailei Ma, Kecheng Zheng, Yuxin Guo, Guosheng Zhao, Yun Zheng, and Xingang Wang. 2024. CoReS: Orchestrating the Dance of Reasoning and Segmentation. *arXiv preprint arXiv:2404.05673* (2024).

[5] Arne Bilberg and Ali Ahmad Malik. 2019. Digital twin driven human–robot collaborative assembly. *CIRP Annals* 68, 1 (2019), 499–502. https://doi.org/10.1016/j.cirp.2019.04.011

[6] Tom B. Brown, Benjamin Mann, Nick Ryder, Melanie Subbiah, Jared Kaplan, Prafulla Dhariwal, Arvind Neelakantan, Pranav Shyam, Girish Sastry, Amanda Askell, et al. 2020. Language Models are Few-Shot Learners. *Advances in Neural Information Processing Systems (NeurIPS)* 33 (2020), 1877–1901. https://doi.org/10.48550/arXiv.2005.14165 arXiv:2005.14165

[7] Yubao Chen. 2017. Integrated and Intelligent Manufacturing: Perspectives and Enablers. *Engineering* 3, 5 (2017), 588–595. https://doi.org/10.1016/J.ENG.2017.04.009

[8] Yi-Chia Chen, Wei-Hua Li, Cheng Sun, Yu-Chiang Frank Wang, and Chu-Song Chen. 2024. SAM4MLLM: Enhance Multi-Modal Large Language Model for Referring Expression Segmentation. arXiv:2409.10542 [cs.AI] https://arxiv.org/abs/2409.10542

[9] Damai Dai, Li Dong, Furu Wei, Bin Xu, Zhifang Liu, and Zhifang Sui. 2023. In-Context Learning: A Comprehensive Survey. *arXiv preprint arXiv:2301.00234* (2023). https://doi.org/10.48550/arXiv.2301.00234

[10] DeepSeek-AI. 2025. DeepSeek-V3 Technical Report. arXiv:2412.19437 [cs.CL] https://arxiv.org/abs/2412.19437

[11] Hao Ding, Lalithkumar Seenivasan, Benjamin D. Killeen, Sue Min Cho, and Mathias Unberath. 2024. Digital twins as a unifying framework for surgical data science: the enabling role of geometric scene understanding. *Artificial Intelligence Surgery* 4, 3 (2024). https://doi.org/10.20517/ais.2024.16

[12] Vlad Fomenko, Han Yu, Jongho Lee, Stanley Hsieh, and Weizhu Chen. 2024. A Note on LoRA. arXiv:2404.05086 [cs.LG] https://arxiv.org/abs/2404.05086

[13] Edward Glaessgen and David Stargel. 2012. The digital twin paradigm for future NASA and U.S. air force vehicles. https://doi.org/10.2514/6.2012-1818

[14] Edward Glaessgen and David Stargel. 2012. The digital twin paradigm for future NASA and U.S. air force vehicles. https://doi.org/10.2514/6.2012-1818

[15] Edward J. Hu, Yelong Shen, Phillip Wallis, Zeyuan Allen-Zhu, Yuanzhi Li, Shean Wang, Lu Wang, and Weizhu Chen. 2021. LoRA: Low-Rank Adaptation of Large Language Models. *arXiv preprint arXiv:2106.09685* (2021). https://doi.org/10.48550/arXiv.2106.09685

[16] Baidu Inc. 2025. ERNIE Bot (Wenxin Yiyan). https://yiyan.baidu.com/

[17] Laurynas Karazija, Iro Laina, and Christian Rupprecht. 2021. ClevrTex: A Texture-Rich Benchmark for Unsupervised Multi-Object Segmentation. arXiv:2111.10265 [cs.CV] https://arxiv.org/abs/2111.10265

[18] Alexander Kirillov, Eric Mintun, Nikhila Ravi, Hanzi Mao, Chloe Rolland, Laura Gustafson, Tete Xiao, Spencer Whitehead, Alexander C. Berg, Wan-Yen Lo, Piotr Dollár, and Ross Girshick. 2023. Segment Anything. arXiv:2304.02643 [cs.CV] https://arxiv.org/abs/2304.02643

[19] Xin Lai, Zhuotao Tian, Yukang Chen, Yanwei Li, Yuhui Yuan, Shu Liu, and Jiaya Jia. 2024. LISA: Reasoning Segmentation via Large Language Model. In *Proceedings of the IEEE/CVF Conference on Computer Vision and Pattern Recognition (CVPR)*. 9579–9589.

[20] Junnan Li, Dongxu Li, Caiming Xiong, and Steven C. H. Hoi. 2022. BLIP: Bootstrapping Language-Image Pre-training for Unified Vision-Language Understanding and Generation. In *Proceedings of the IEEE/CVF Conference on Computer Vision and Pattern Recognition (CVPR)*. 1288–1300. https://doi.org/10.1109/CVPR52688.2022.00135

[21] Chang Liu, Henghui Ding, and Xudong Jiang. 2023. GRES: Generalized Referring Expression Segmentation. arXiv:2306.00968 [cs.CV] https://arxiv.org/abs/2306.00968

[22] Zheng Liu, Norbert Meyendorf, and Nezih Mrad. 2018. The role of data fusion in predictive maintenance using digital twin. *AIP Conference Proceedings* 1949, 1 (04 2018), 020023. https://doi.org/10.1063/1.5031520 arXiv:https://pubs.aip.org/aip/acp/article-pdf/doi/10.1063/1.5031520/13848976/020023_1_online.pdf

[23] Junhua Mao, Jonathan Huang, Alexander Toshev, Oana Camburu, Alan Yuille, and Kevin Murphy. 2016. Generation and Comprehension of Unambiguous Object Descriptions. arXiv:1511.02283 [cs.CV] https://arxiv.org/abs/1511.02283

[24] Matthias Minderer, Alexey Gritsenko, and Neil Houlsby. 2024. Scaling Open-Vocabulary Object Detection. arXiv:2306.09683 [cs.CV] https://arxiv.org/abs/2306.09683

[25] Neda Mohammadi and John E. Taylor. 2017. Smart city digital twins. In *2017 IEEE Symposium Series on Computational Intelligence (SSCI)*. 1–5. https://doi.org/10.1109/SSCI.2017.8285439

[26] OpenAI. 2024. GPT-4o-mini: Lightweight Multimodal Language Model. https://platform.openai.com/docs/models/gpt-4o-mini Version: gpt-4o-mini-2024-07-18.

[27] OpenAI. 2024. GPT-4o: Multimodal Language Model with Omni Capabilities. https://platform.openai.com/docs/models/gpt-4o Version: gpt-4o-2024-05-13.

[28] Alec Radford, Jong Wook Kim, Chris Hallacy, Aditya Ramesh, Gabriel Goh, Sandhini Agarwal, Girish Sastry, Amanda Askell, Pamela Mishkin, Jack Clark, et al. 2021. CLIP: Connecting Text and Images. *arXiv preprint arXiv:2103.00020* (2021). https://arxiv.org/abs/2103.00020 Foundational work on vision-language pretraining.

[29] Meta AI Research. 2024. Llama 3.3-70B-Instruct: A Cost-Efficient Open Foundation Model. https://huggingface.co/meta-llama/Llama-3.3-70B-Instruct

[30] Hamid Rezatofighi, Nathan Tsoi, JunYoung Gwak, Amir Sadeghian, Ian Reid, and Silvio Savarese. 2019. Generalized Intersection over Union: A Metric and A Loss for Bounding Box Regression. In *Proceedings of the IEEE/CVF Conference on Computer Vision and Pattern Recognition (CVPR)*. 658–666. https://doi.org/10.1109/CVPR.2019.00075

[31] Hongchao Shu, Ruixing Liang, Zhaoshuo Li, Anna Goodridge, Xiangyu Zhang, Hao Ding, Nimesh Nagururu, Manish Sahu, Francis X. Creighton, Russell H. Taylor, Adnan Munawar, and Mathias Unberath. 2023. Twin-S: A Digital Twin for Skull-base Surgery. arXiv:2211.11863 [cs.HC] https://arxiv.org/abs/2211.11863

[32] Hugo Touvron et al. 2023. LLaMA: Open and Efficient Foundation Language Models. *arXiv preprint arXiv:2302.13971* (2023). https://arxiv.org/abs/2302.13971

[33] Junchi Wang and Lei Ke. 2024. LLM-Seg: Bridging Image Segmentation and Large Language Model Reasoning. In *Proceedings of the IEEE/CVF Conference on Computer Vision and Pattern Recognition (CVPR) Workshops*. 1765–1774.

[34] Wenhai Wang, Zhe Chen, Xiaokang Chen, Jiannan Wu, Xizhou Zhu, Gang Zeng, Ping Luo, Tong Lu, Jie Zhou, Yu Qiao, and Jifeng Dai. 2023. VisionLLM: Large Language Model is also an Open-Ended Decoder for Vision-Centric Tasks. arXiv:2305.11175 [cs.CV] https://arxiv.org/abs/2305.11175

[35] XuDong Wang, Shaolun Zhang, Shufan Li, Kehan Li, Konstantinos Kallidromitis, Yusuke Kato, Kazuki Kozuka, and Trevor Darrell. 2025. SegLLM: Multi-round Reasoning Segmentation with Large Language Models. In *The Thirteenth International Conference on Learning Representations*. https://openreview.net/forum?id=Pm1NXHgzyf

[36] Cong Wei, Haoxian Tan, Yujie Zhong, Yujiu Yang, and Lin Ma. 2024. LaSagnA: Language-based Segmentation Assistant for Complex Queries. arXiv:2404.08506 [cs.CV] https://arxiv.org/abs/2404.08506

[37] Jason Wei, Xuezhi Wang, Dale Schuurmans, Maarten Bosma, Ed Chi, Quoc Le, and Denny Zhou. 2022. Chain-of-Thought Prompting Elicits Reasoning in Large Language Models. *Advances in Neural Information Processing Systems (NeurIPS)* 35 (2022), 24824–24837.

[38] Zhuofan Xia, Dongchen Han, Yizeng Han, et al. 2024. GSVA: Generalized Segmentation via Multimodal Large Language Models. In *Proceedings of the IEEE/CVF Conference on Computer Vision and Pattern Recognition (CVPR)*. 3858–3869.

[39] Daoguang Yang, Hamid Karimi, Okyay Kaynak, and Shen Yin. 2021. Developments of digital twin technologies in industrial, smart city and healthcare sectors: a survey. *Complex Engineering Systems* 1 (09 2021). https://doi.org/10.20517/ces.2021.06

[40] Senqiao Yang, Tianyuan Qu, Xin Lai, et al. 2024. LISA++: An Improved Baseline for Reasoning Segmentation with Large Language Model. arXiv:2312.17240 [cs.CV] https://arxiv.org/abs/2312.17240

[41] Yuqi Yang, Peng-Tao Jiang, Jing Wang, Hao Zhang, Kai Zhao, Jinwei Chen, and Bo Li. 2024. Empowering Segmentation Ability to Multi-modal Large Language Models. arXiv:2403.14141 [cs.CV] https://arxiv.org/abs/2403.14141

[42] Shunyu Yao, Jeffrey Zhao, Dian Yu, Nan Du, Izhak Shafran, Karthik Narasimhan, and Yuan Cao. 2023. ReAct: Synergizing Reasoning and Acting in Language Models. In *International Conference on Learning Representations (ICLR)*.

[43] Licheng Yu, Patrick Poirson, Shan Yang, Alexander C. Berg, and Tamara L. Berg. 2016. Modeling Context in Referring Expressions. In *Proceedings of the European Conference on Computer Vision (ECCV)*. 69–85. https://doi.org/10.1007/978-3-319-46475-6_5 Extended work on RefCOCO/+ datasets.

[44] Zhaohui Zheng, Ping Wang, Wei Liu, Jinze Li, Rongguang Ye, and Dongwei Ren. 2020. Distance-IoU Loss: Faster and Better Learning for Bounding Box Regression. *Proceedings of the AAAI Conference on Artificial Intelligence* 34, 07 (2020), 12993–13000. https://doi.org/10.1609/aaai.v34i07.6999

[45] Denny Zhou, Hong Liu, Jaehoon Lee, and Aviral Kumar. 2024. Chain-of-Thought Reasoning without Prompting: Mining the Intrinsic Reasoning Abilities of Language Models. *arXiv preprint* (2024). https://doi.org/10.48550/arXiv.2408.03314